Original Research

Obesity, independent of diet, drives lasting effects on intestinal epithelial stem cell proliferation in mice

Weinan Zhou[1], Elizabeth A Davis[2] and Megan J Dailey[1,2]

[1]Department of Animal Sciences, University of Illinois at Urbana-Champaign, Urbana, IL 61801, USA; [2]Neuroscience Program, University of Illinois at Urbana-Champaign, Urbana, IL 61801, USA

Corresponding author: Weinan Zhou. Email: wzhou29@illinois.edu

Impact statement

This study investigates whether obesity or the type/amount of diet differentially alters the proliferation, differentiation, growth, and function of the intestinal epithelial tissue. Although diet-induced obesity is known to alter the growth and function of the epithelium *in vivo* and cause lasting effects in intestinal epithelial stem cells (IESCs) *in vitro*, we are the first to tease apart the separate contributions of obesity versus the type/amount of diet in these processes. We found that high-fat diet (HFD)-induced obesity, independent of the HFD, drives lasting effects on IESC proliferation and differentiation into goblet cells, which may contribute to the growth of the epithelium. In addition, there is an interaction of obesity, type of diet, and availability of the diet (PF versus ad libitum) on the function of enterocytes. Identification of the factors driving the epithelial changes may provide new therapeutic strategies to control altered tissue growth and function associated with obesity.

Abstract

The intestinal epithelium plays an essential role in nutrient absorption, hormone release, and barrier function. Maintenance of the epithelium is driven by continuous cell renewal by intestinal epithelial stem cells located in the intestinal crypts. Obesity affects this process and results in changes in the size and function of the tissue. Because both the amount of food intake and the composition of the diet are contributing factors to developing and maintaining obesity, it is necessary to tease apart the separate contributions of obesity versus the type/amount of diet in driving the epithelial changes. C57BL/6J mice were fed a 60% high-fat diet versus a 10% low-fat diet for three months. A pair fed group was included (mice were fed with high-fat diet, but in equal kcal as that eaten by the low-fat diet- fed mice to keep them lean). We investigated the differences in (1) crypt-villus morphology *in vivo*, (2) the number and function of differentiated epithelial cell types *in vivo*, and (3) lasting effects on intestinal epithelial stem cell proliferation and growth *in vitro*. We found that high-fat diet-induced obesity, independent of the high-fat diet, increased crypt depth, villus height, the number of intestinal epithelial stem cells and goblet cells *in vivo*, and enhanced the size of the enterospheres developed from isolated IESCs *in vitro*. In addition, there is an interaction of obesity, type of diet, and availability of the diet (pair fed versus *ad libitum*) on protein and mRNA expression of alkaline phosphatase (an enzyme of enterocytes). These results suggest that high-fat diet-induced obesity, independent of the high-fat diet, induces lasting effects on intestinal epithelial stem cell proliferation, and drives the differentiation into goblet cells, but an interaction of obesity and diet drives alterations in the function of the enterocytes.

Keywords: Obesity, diet, intestine, stem cell, proliferation, epithelial function

***Experimental Biology and Medicine* 2018; 243: 826–835. DOI: 10.1177/1535370218777762**

Introduction

The intestinal epithelium plays an essential role in nutrient absorption, satiety hormone release, and immune barrier function. Maintenance of the epithelium is driven by continuous cell renewal by intestinal epithelial stem cells (IESCs) located in the intestinal crypts.[1] IESCs give rise to progenitor cells, and then progenitor cells differentiate into mature intestinal epithelial cell types (e.g. enterocytes, enteroendocrine cells, goblet cells and Paneth cells) as they migrate through the crypt-villus axis. Obesity affects this process and results in changes in the size and cellular make-up of the tissue.[2] In particular, obesity increases IESC number and proliferation, total epithelial cell number, villus height or crypt depth *in vivo*.[3–6] Moreover, diet-induced obesity causes lasting effects in IESCs, such that isolated IESCs from obese compared to lean mice grow at different rates *in vitro*.[3,4] These findings suggest that obesity may alter the proliferation, growth, and function of the

intestinal epithelial tissue through the modulation of somatic stem cells.

Previous studies investigating the effect of obesity on the proliferation of IESCs used a diet-induced obese mouse model that is limited to comparing a high-fat diet (HFD)-fed versus chow-fed mice.[3,4] Although chow is a low-fat diet (LFD) that will result in a lean phenotype when consumed *ad libitum* in rodents, chow-fed mice do not eat the same kilocalorie (kcal) amount as the HFD-fed mice.[7–11] In addition, the ingredients and composition of these diets vary greatly (e.g. sugar, fiber, and protein). Both the amount of food intake and the composition of the diet are factors that may lead to alterations in intestinal epithelial growth and function independent of the body weight differences between groups. In order to control for these factors, we chose to use an LFD that has the same ingredients as the HFD with only the amount of fat or carbohydrate varied, and included a pair fed (PF) group that was fed the HFD, but in equal kilocalories as that eaten by the LFD group. Using this model allows us to tease apart the separate contributions of obesity versus the type/amount of diet in altering proliferation, growth, and function of the intestinal epithelial tissue. Mice were equally divided into three groups and fed (1) a 60% HFD *ad libitum*, (2) a 10% LFD fed *ad libitum* or (3) an HFD PF group. After three months on the respective diets, mice were euthanized and the crypt depth, villi height, the number of different intestinal epithelial cell types and the expression of enzymes or secretory proteins of different intestinal epithelial cell types were measured *in vivo*, whereas the lasting effects on IESC proliferation and epithelial growth were measured *in vitro*.

Methods

Animals

Male C57BL/6J mice at 10-weeks-old were obtained from the Jackson Laboratory (Bar Harbor, ME; $N = 24$). Mice were individually housed in modified shoebox cages with a raised woven wire platform and lined with brown kraft paper for collection and measurement of food spillage. Mice were acclimated to the housing for one week with *ad libitum* access to tap water and laboratory chow (Tecklad 22/5, Tecklad Diets, Madison, WI) on a 12:12 light:dark cycle in a climate-controlled room (22 ± 1°C and 60% relative humidity). All procedures were approved by the Institutional Animal Care and Use Committee at the University of Illinois at Urbana-Champaign.

Following the one week acclimation, mice were fed an HFD or an LFD for three months. The HFD and control groups were as follows: (1) 60% HFD *ad libitum* fed (Research Diets D12492), (2) 10% LFD *ad libitum* fed (Research Diets D12450J), and (3) 60% HFD PF group (fed a HFD, but in equal kcal as that eaten by the LFD fed animals to keep them lean), $n = 8$ per group. It is not possible to include an LFD that eats the same kcal amount as the HFD ad libitum group without using a transgenic mouse or lesioning the hypothalamus to induce hyperphagia of the LFD. Mice were weighed weekly and food intake was measured daily. Mice in HFD PF group were given an equal kcal of the food eaten by the LFD-fed mice a day later than other groups.

After three months, mice were killed by decapitation under isoflurane anesthesia (Henry Schein Animal Health, Dublin, OH). A subset of the mice ($n = 5$ per group) were used for histology or qPCR. A power analysis (G×Power 3.1.9.2) based on previously published data investigating the lasting effect of diet-induced obesity on IESC growth *in vitro* and epithelial changes *in vivo* show that to achieve a power = 0.8 and a type I error of 0.05, an $n = 3$ per group for *in vitro* experiments and an $n = 5$ per group for *in vivo* analysis are needed.[3,4] The intestine was exposed, and tissue was collected from the duodenum, jejunum, ileum, and colon as previously described.[12] Briefly, to ensure that we are collecting similar segments of the intestine for analysis between animals, we measured from the pyloric sphincter, discarded the first 1 cm, and then collected two 5 mm samples to be processed for histology or qPCR. We then measured from the cecum, discarded the first 1 cm, and then collected two 5 mm segments of the ileum or colon. From the remaining jejunal segment, we measured from the middle and collected two 5 mm segments to be processed similarly to the duodenal and ileal segments. For histology, each of the 5 mm intestinal segments were fixed in 10% neutral-buffered formalin for 24 h at RT and then stored in 70% ETOH at RT prior to paraffin embedding. For qPCR, each of the 5 mm intestinal segments was stored in RNAlater stabilization solution (Invitrogen, Carlsbad, CA) at −80°C prior to RNA extraction. Another subset of mice ($n = 3$ per group) were used for isolation and culture of IESCs. For these mice, the entire small intestine was harvested for immediate IESC isolation.

IESC isolation

IESCs were isolated as previously described.[13,14] Briefly, the entire small intestine was harvested, opened longitudinally, and washed with cold 1× PBS to remove luminal contents. The villi were scraped off with a coverslip. The tissue was cut into 2–4 mm pieces with scissors and washed 5–10 times with cold 1× PBS until the supernatant was almost clear. Tissue fragments were incubated with 2 mM EDTA (Fisher Scientific, Pittsburgh, PA) and gently rocked at 4°C for 30 min. After removal of EDTA, tissue fragments were washed with 1× PBS three times. The supernatant was then collected and passed through a 70-μm cell strainer (Corning, Corning, NY) and centrifuged at 300*g* at 4°C for 5 min. The cell pellet was resuspended with single cell dissociation medium (Advanced DMEM/F12 [Gibco, Grand Island, NY], 2 mM GlutaMax [Gibco, Grand Island, NY], 10 mM HEPES [Gibco, Grand Island, NY], 100 U/mL Penicillin–Streptomycin [Gibco, Grand Island, NY], 1× N2 [Gibco, Grand Island, NY], 1× B27 [Gibco, Grand Island, NY], 10 μM Y-27632 [Sigma-Aldrich, St. Louis, MO]) at 37°C for 45 min. During incubation, the cell suspension was pipetted every 10 min. Dissociated cells were passed through a 40-μm cell strainer (pluriSelect, Leipzig, Germany), followed by a 20-μm cell strainer (pluriSelect, Leipzig, Germany) and centrifuged at 300*g* at 4°C for

5 min. The pellet was then resuspended with staining medium (Advanced DMEM/F12, 2 mM GlutaMax, 10 mM HEPES, 100 U/mL Penicillin–Streptomycin, 10 μM Y-27632, 0.5 mM N-Acetyl-L-cysteine [Sigma-Aldrich, St. Louis, MO]), and stained with antibodies including CD45-FITC (1:100; eBioscience, San Diego, CA), CD44-PE/Cy5 (1.5:100; BioLegend, San Diego, CA), CD24-eFluor 450 (1.25:100; eBioscience, San Diego, CA), CD166-PE (1.5:100; R&D Systens, Minneapolis, MN), and GRP78 (0.5:100; Sigma-Aldrich, St. Louis, MO) at 4°C for 30 min followed by secondary antibody, goat anti-rabbit IgG, F(ab')2-APC (1:100; Santa Cruz Biotechnology, Dallas, TX), straining for another 30 min at 4°C, and IESCs were isolated as $CD45^{-}CD44^{+}CD24^{low}CD166^{medium/low}GPR78^{low/-}$ by fluorescence-activated cell sorting (FACS) with a BD FACS ARIA II sorter into staining medium for following culture. Dead cells were excluded from the FACS with the viability dye propidium iodide (Invitrogen, Carlsbad, CA).

Cell culture

Isolated IESCs were cultured as previously described.[14,15] Briefly, freshly isolated IESCs from each animal were embedded in Matrigel (Corning, Corning, NY) including 1 μM Jagged-1 peptide (Ana Spec, Fremont, CA) at 500 IESCs/10 μL, seeded on 96-well plate (replicates of three wells per animal), and incubated in IESC culture medium (Advanced DMEM/F12 containing 2 mM GlutaMax, 10 mM HEPES, 100 U/mL Penicillin–Streptomycin, 1×N2, 1×B27, 1 mM N-Acetyl-L-cysteine, 50 ng/mL EGF [Gibco, Grand Island, NY], 100 ng/mL Noggin [PeproTech, Rocky Hill, NJ], 500 ng/mL R-Spondin-1 [PeproTech, Rocky Hill, NJ], 3 μM CHIR99021 [Sigma-Aldrich, St. Louis, MO] and 1 mM valproic acid [Sigma-Aldrich, St. Louis, MO]). Two inhibitors of differentiation (CHIR99021 and valproic acid) were used to maintain IESCs in a self-renewing and undifferentiated state,[15] which allow for us to assess the lasting effect of obesity or the type/amount of diet on IESC proliferation without the interference of mixed cell types in previously described IESC culture conditions. Medium was changed every other day. Representative images were captured from day 2 to day 12 post plating using an Axio Vert.A1 inverted microscope (Zeiss, Oberkochen, Germany) fitted with an Axiocam 503 mono camera (Zeiss, Oberkochen, Germany). Enterosphere size was quantified through analysis of captured images at 10× magnification using ImageJ software (NIH, Bethesda, MD).

Histology

Formalin fixed tissue sections were embedded using paraffin and cut on a microtome at 5 μm thickness and mounted onto charged glass microscope slides. For crypt-villus morphology, tissue sections were deparaffinized in xylenes followed by a series of graded ethanol, then rinsed in deionized water. Intestinal sections were counterstained in hematoxylin (Fisher HealthCare, Houston, TX) and dehydrated in a series of graded ethanol followed by xylenes. Slides were mounted with Permount mounting media (Fisher Scientific, Pittsburgh, PA) and stored at RT.

For immunohistochemical processing for Olfactomedin-4 (Olmf4; an IESC marker) and Chromogranin A (an enteroendocrine cell marker), after deparaffinizing slides as described above, antigen retrieval was performed by immersing the slides in the sodium citrate buffer (10 mM sodium citrate hydrochloride [Fisher Scientific, Pittsburgh, PA] and 0.05% Tween 20 [Sigma-Aldrich, St. Louis, MO] diluted in distilled water, pH 6.0) for 20 min in a water bath at 95°C, then allowed to cool, while still immersed in the sodium citrate buffer solution for 30 min at RT. Slides were rinsed between each step in 1× PBS. Slides were incubated in blocking solution (3% Normal Donkey Serum [Jackson ImmunoResearch, West Grove, PA] and 0.3% Triton X-100 [Sigma-Aldrich, St. Louis, MO] diluted in 1× PBS) for 1 h at RT. Sections were incubated overnight at 4°C in the following primary antibodies diluted in the blocking solution: Olmf4 (1:400; Cell Signaling Technology, Danvers, MA), Chromogranin A (1:1,000; Abcam, Cambridge, United Kingdom). Sections were incubated in a donkey anti-rabbit biotin-conjugated IgG (H&L) secondary antibody (1:500, Jackson ImmunoResearch, West Grove, PA) diluted in 1× PBS for 1 h at RT. Sections were then incubated in an avidin-biotin complex (Vector Laboratories, Burlingame, CA) for 30 min at RT. A diaminobenzidine-hydrogen peroxidase reaction was performed using a substrate kit (Vector Laboratories, Burlingame, CA). Slides were dehydrated and mounted as described above.

For Periodic Acid Schiff staining of mucins (a goblet cell marker) and Paneth cell granules (a Paneth cell marker), after deparaffinizing slides as described above, slides were immersed in 0.5% Periodic Acid (Newcomer Supply, Middleton, WI) for 10 min at RT and washed in distilled water. Sides were then immersed in Schiff reagent (Newcomer Supply, Middleton, WI) for 30 min at RT and rinsed in 0.55% potassium metabisulfite (Fisher Scientific, Pittsburgh, PA) for 30 s and followed by washing in warm running tap water for 10 min. Slides were counterstained in hematoxylin, dehydrated and mounted as described above.

For staining of alkaline phosphatase (an enterocyte marker), after deparaffinizing slides as described above, slides were immersed in alkaline phosphatase substrate working solution (Vector Laboratories, Burlingame, CA) for 25 min. Slides were then washed in 100 mM Tris hydrochloride (PH 8.2; Fisher Scientific, Pittsburgh, PA) for 5 min and followed by washing in running distilled water for 5 min. Slides were dehydrated and mounted as described above.

Intestinal tissues sections were visualized using a NanoZoomer Digital Pathology (NDP) System (Hamamatsu, Hamamatsu City, Japan) using a 40× objective and NDP Scan software. Crypt depth and villus height of three intestinal cross sections (4 crypts or villi per section) from each segment of the intestine (duodenum, jejunum, ileum and colon) per mouse were measured using NDP View 2 software. The number of Olmf4-postive IESCs, Chromogranin A-positive enteroendocrine cells, Periodic Acid Schiff-positive goblet cells, and Periodic Acid Schiff-positive Paneth cells of three intestinal cross sections (three crypts or villi per section) from the jejunum per mouse was measured using NDP View 2 software.

The expression of alkaline phosphatase was determined by measuring relative intensity of alkaline phosphatase staining of three intestinal cross sections (three villi per section) from the jejunum per mouse were measured using ImageJ software.

qPCR

In order to investigate whether obesity or the type/amount of diet alters the function of differentiated intestinal epithelial cell types, we measured the expression of alkaline phosphatase (an enzyme of enterocyte regulating lipid absorption and barrier function),[16] lysozyme (an antimicrobial protein secreted by Paneth cells),[17] chromogranin A (a protein secreted by enteroendocrine cells, which facilitates the release of different peptide hormones through controlling dense-core secretory granule biogenesis),[18,19] and mucin 2 (the major secretory mucin secreted by goblet cells).[20] Total RNA was extracted from tissue using RNeasy Plus Mini Kit (Qiagen, Hilden, Germany). RNA was reverse transcribed into cDNA using QuantiTect Reverse Transcription Kit (Qiagen, Hilden, Germany). qPCR was performed with TaqMan Universal PCR Master Mix (Applied Biosystems, Foster City, CA) and TaqMan probes (Applied Biosystems, Foster City, CA) using Applied Biosystems QuantStudio™ 7 Flex Real-Time PCR System. Negative reverse-transcribed samples were generated and all reactions were carried out in triplicate. The following TaqMan probes were used: Alpi: Mm01285814_g1, Lyz1: Mm00657323_m1, Chga: Mm00514341_m1, Muc2: Mm01276696_m1, and GAPDH: Mm99999915_g1. To determine relative expression values, the $2^{-\Delta\Delta Ct}$ method was used, where triplicate Ct values for each sample were averaged and subtracted from those derived from GAPDH.

Data analysis

Data are expressed as Mean ± SEM. For measurement of body weight and daily food intake, differences between groups were analyzed using a two-way RM ANOVA. Differences between groups for average daily food intake were analyzed using a Student's *t* test. For measurements of crypt depth, villus height, number of different intestinal cell types, the relative intensity of alkaline phosphatase staining and qPCR, differences between groups for each segment were analyzed using a one-way ANOVA. For measurement of enterosphere size, differences between groups at each time points were analyzed using a one-way ANOVA. Fisher's LSD *post hoc* tests were used where appropriate. $P < 0.05$ was considered statistically significant.

Results

Body weight and food intake

Body weight and food intake were increased in the HFD-fed mice compared with the LFD and HFD PF groups (Figure 1(a) to (c); $P < 0.05$).

Intestinal crypt and villus morphometry

Crypt depth and villus height in the duodenum and jejunum were increased in the HFD-fed mice compared with the LFD and HFD PF groups (Figure 2(b) and (c); $P < 0.05$), but no differences were found in the ileum and colon (Figure 2(b) and (c)).

Number of intestinal epithelial cell types

The number of Olmf4-positive IESCs and Periodic Acid Schiff-positive goblet cells in the jejunum was increased in the HFD-fed mice compared with the LFD and HFD PF groups (Figure 3(b) and (h); $P < 0.05$). There were no differences in the number of Periodic Acid Schiff-positive Paneth cells and Chromogranin A-positive enteroendocrine cells in the jejunum between the HFD, HFD PF, or LFD groups (Figure 3(d) and (f)).

Expression of intestinal enzymes or secretory proteins

The protein levels of alkaline phosphatase (a marker for enterocytes) were highest in the HFD PF group in the jejunum (Figure 3(j); $P < 0.05$). Specifically, alkaline phosphatase levels in the HFD PF group were increased compared with the HFD and LFD groups (Figure 3(j); $P < 0.05$). Alkaline phosphatase levels were also increased in the HFD compared with the LFD group (Figure 3(j); $P < 0.05$). Gene expression of alkaline phosphatase was highest in the HFD PF group, with significant increases in the duodenum and jejunum (Figure 4(d); $P < 0.05$). Specifically, alkaline phosphatase expression in the HFD PF group was increased in the duodenum compared with the HFD group and in the jejunum compared with the HFD and LFD groups (Figure 4(d); $P < 0.05$). Alkaline phosphatase expression was also increased in the HFD compared with the LFD group, but only in the jejunum (Figure 4(d); $P < 0.05$). There were no differences in the gene expression of lysozyme (a marker for Paneth cells), chromogranin A (a marker for enteroendocrine cells) and mucin 2 (a marker for goblet cells) between the HFD, HFD PF, or LFD groups (Figure 4(a) to (c)).

IESC proliferation in culture

The size of the enterospheres that developed from IESCs isolated from HFD-fed mice was increased compared with those from HFD PF group and LFD group on days 11 and 12 post plating (Figure 5(b); $P < 0.05$). There were no differences in the number of enterospheres developed from IESCs isolated from any group (data not shown).

Discussion

The aim of these experiments was to investigate whether obesity or the type/amount of diet differentially alters the proliferation, growth, and function of the intestinal epithelial tissue. The major findings were: (1) HFD-induced obesity, independent of the HFD, increased crypt depth and villus height in the duodenum and jejunum of intestine *in vivo*, (2) HFD-induced obesity, independent of the HFD, induced increases in the number of IESCs and goblet cells

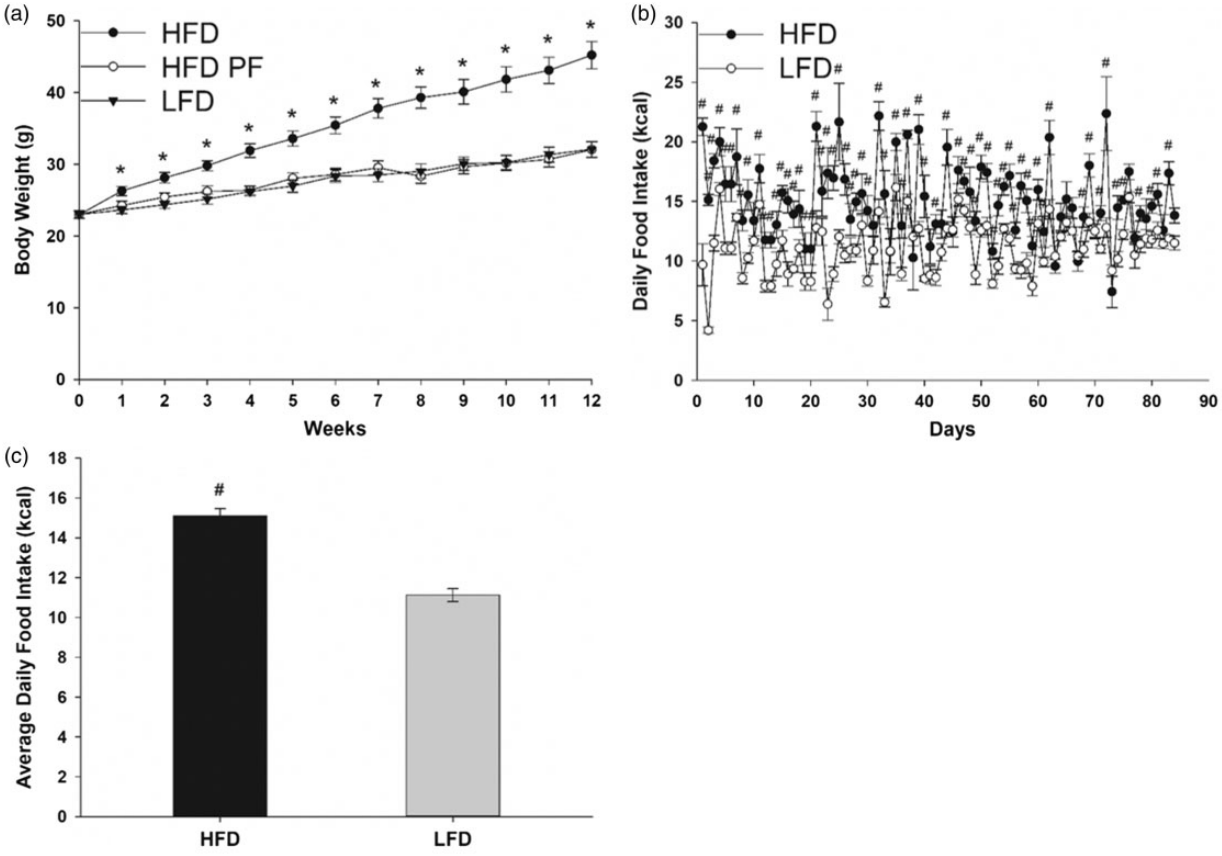

Figure 1. Body weight (a), daily food intake (b) and average daily food intake (c) of mice fed with HFD or LFD for three months. Data are expressed as Mean ± SEM ($n = 8$). * indicates significant different between HFD and HFD PF groups and between HFD and LFD groups at that time point, $P < 0.05$. # indicates significantly different between HFD and LFD groups at that time point, $P < 0.05$.

in the jejunum *in vivo*, (3) HFD-induced obesity, independent of the HFD, enhanced IESC proliferation and growth *in vitro*, and (4) there was an interaction of obesity, the type of diet (HFD), and availability of the diet (PF versus *ad libitum*) on the function of enterocytes in the duodenum and jejunum of intestine *in vivo*.

Consistent with previous findings,[3,5,6,21] our results showed that HFD-induced obesity leads to a growth of the epithelium as measured by increases in crypt depth and villus height, and this increase in epithelial mass is reflected by an increase in the number of IESCs and goblet cells. We showed for the first time that this effect was not driven by the HFD alone and occurs even when an LFD of a similar composition is used as a control condition (as opposed to a chow-fed group). Because the intestinal epithelial cells are the first point of contact with ingested food and prepare the body for the nutrients that are entering the system, it makes sense that their cellular make-up would be comprised of cells that would be best suited for the digestion of a diet that is maintained across time. The high adaptability of the epithelium to change its cellular make-up is likely due to a coordinated effort of the presence and nature of the distinct food components (e.g. proteins, lipids, carbohydrates) in the lumen of the intestinal tract mixed with signals from the basal surface of the tissue (e.g. hormonal, neural). These signals likely direct the IESCs to proliferate and direct the progenitor cells at the crypt-villus axis to differentiate into the functional cells needed. Moreover, this obesity-induced tissue growth is pronounced in the proximal, but not the distal intestine. Although we find differences in the HFD-induced obesity effect between the proximal and distal axis, there is data to support the idea that the IESCs are not intrinsically different between the intestinal segments and, instead, proliferation and differentiation along the proximal to distal axis are driven by the local niche environment at each segment. Intestinal transposition studies where duodenal, jejunal or ileal segments are transposed with each other show that the proliferation, total number of epithelial cells, and villus height are determined by the environment and not an intrinsic property of the crypts that contain the IESCs at each segment.[22] For example, the short villi normally seen in ileal segments quickly grow long when transplanted into the duodenum or vice versa.[22] The function of transposed or transplanted segments can also be regained.[22] In addition, we find that isolated crypts from the duodenum, jejunum, ileum, or colon grown under the same conditions *in vitro* will produce all of the same types of daughter cells even though they do not produce these *in vivo* (unpublished observations). For example, enteroendocrine cell types typically vary along the proximal to distal axis of the intestinal tract with I cells in the proximal and L cells

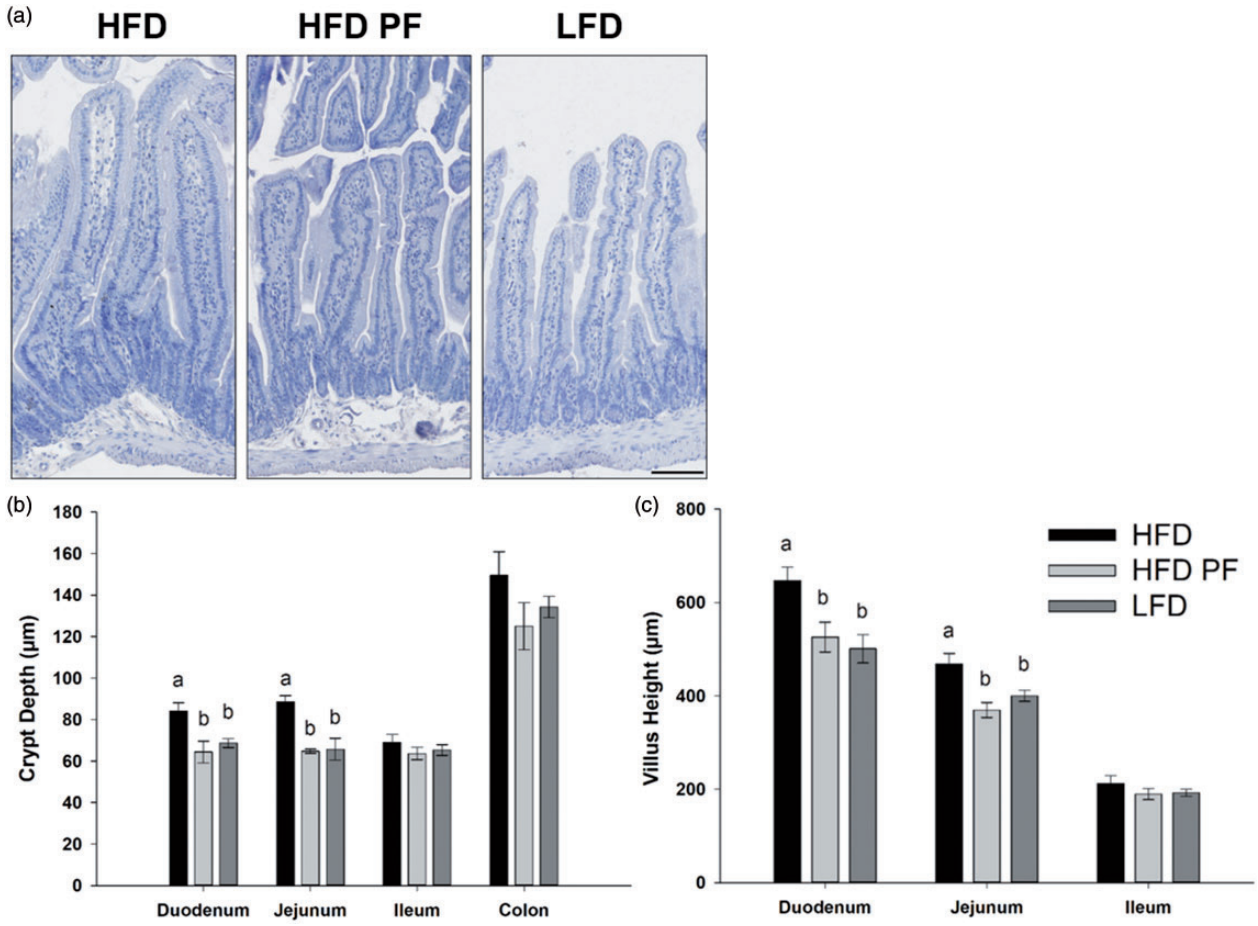

Figure 2. Representative images of hematoxylin stained crypt-villus morphology in the jejunum (a), and quantification of crypt depth (b) and villus height (c) in intestinal segments (duodenum, jejunum, ileum, and colon) collected from mice fed with HFD or LFD. Scale bar, 100 μm. Data are expressed as Mean ± SEM ($n = 5$). Means with different letters indicate significantly different in each intestinal segment, $P < 0.05$. (A color version of this figure is available in the online journal.)

in the distal intestine. We find that both cell types are produced in the same enterospheres *in vitro*, regardless from where the crypts were isolated along the intestinal axis (unpublished observations). Thus, it is likely that the environment along the intestinal axis drives the differences in response to HFD-induced obesity and not intrinsic differences between the IESCs from each intestinal segment. There is likely a coordinated effort of the presence and nature of the distinct food components and enzymes in the lumen of each segment of the intestinal tract mixed with signals from the basal surface of the tissue.

We found that there is an interaction of obesity, the type of diet, and availability of the diet (PF versus *ad libitum*) on protein and mRNA expression of alkaline phosphatase, but not the expression of markers for other differentiated cell types. Moreover, this effect is pronounced in the proximal, but not the distal segments of intestine. Alkaline phosphatase is a brush border protein that has a number of activities, including the hydrolysis of various substrates, and participates in a rate-limiting step regulating fat absorption.[16,23] It is expressed exclusively in villus-associated enterocytes and can be released into the lumen or circulation.[24] Although often used as a marker for the number of enterocytes, it is likely a better marker for the activity occurring in the enterocytes. Alkaline phosphatase is increased during fat absorption and is higher in animals maintained on a high fat diet.[25] Just as we have found, though, there are dissimilar results between groups of animals due to the differences in the amount eaten or fatty acid composition of the HFD.[16,26–29] The role of alkaline phosphatase in HFD-driven effects is further complicated by data showing that alkaline phosphatase levels are positively correlated with obesity,[30,31] but that high levels of alkaline phosphatase can protect against HFD-induced obesity and the development of type II diabetes.[30,32,33] The distinction for the role of alkaline phosphatase may depend on when the protein is measured in the progression of HFD ingestion, development of obesity and the diabetic condition given that HFD dose-dependent effects on gene expression have been found. It appears that the intestinal epithelium has the capacity to handle increasing levels of dietary fat until a threshold (20% fat), but then progressive adaptations in epithelial activity are more pronounced as dietary fat levels continue to increase above that threshold (from 20% to 30% to 45% fat).[34] We postulate that the HFD-driven increase in alkaline phosphatase in our HFD PF group is attenuated in our HFD group by circulating factors related to obesity. Conversely, there may have

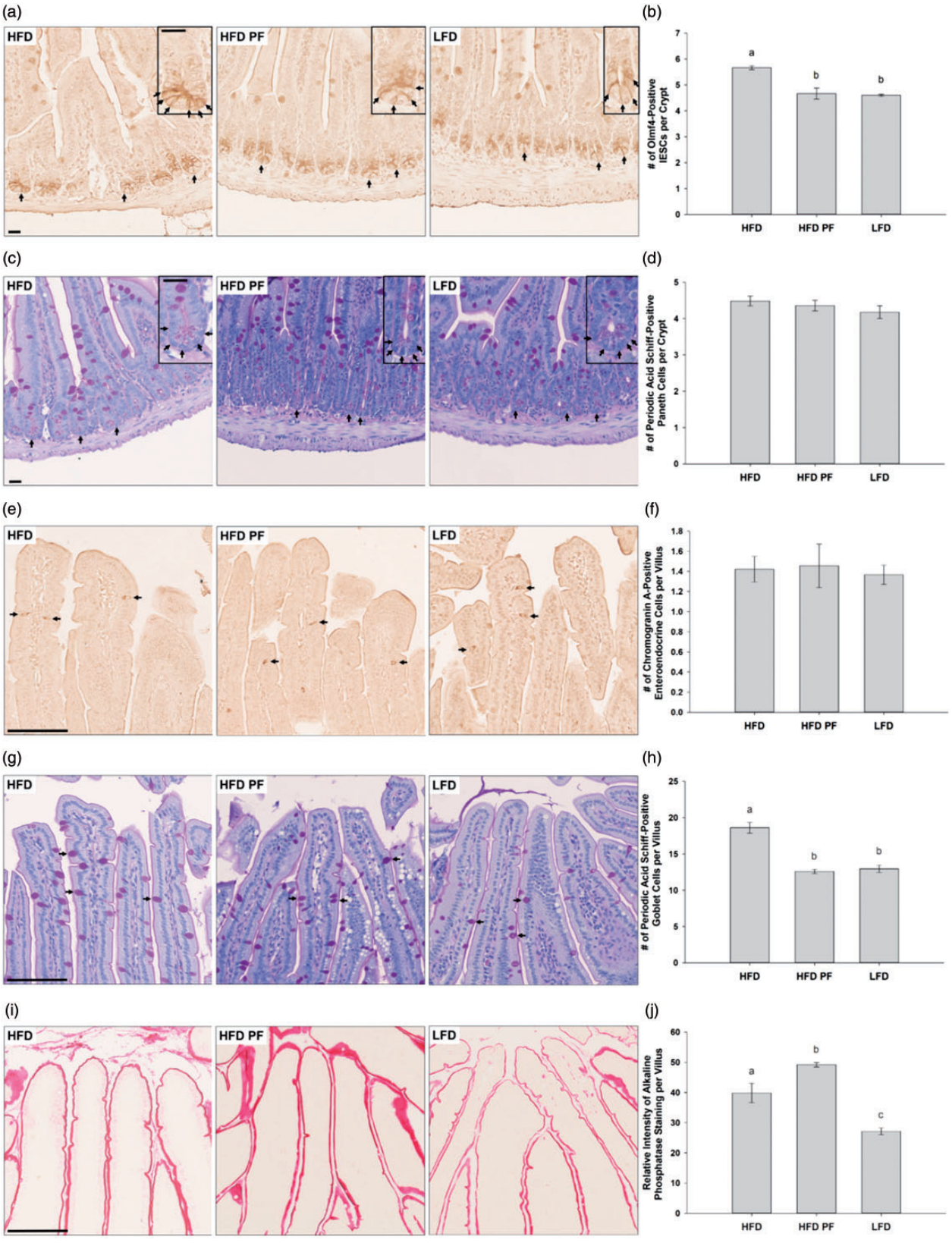

Figure 3. Representative images of the jejunal sections collected from mice fed with HFD or LFD stained with Olmf4 (IESC marker), Scale bar, 20 μm (a), Paneth cell granules (Paneth cell marker), Scale bar, 20 μm (c), Chromogranin A (enteroendocrine cell maker), Scale bar, 100 μm (e), mucins (goblet cell marker), Scale bar, 100 μm (g), and alkaline phosphatase (enterocyte marker), Scale bar, 100 μm (i). Quantification of the number of Olmf4-positive IESCs (b), periodic acid Schiff-positive Paneth cells (d), chromogranin A-positive enteroendocrine cells (f), and periodic acid Schiff-positive goblet cells (h) in the jejunum. Quantification of relative intensity of alkaline phosphatase staining (j). Data are expressed as Mean ± SEM ($n = 5$). Means with different letters indicate significantly different, $P < 0.05$. (A color version of this figure is available in the online journal.)

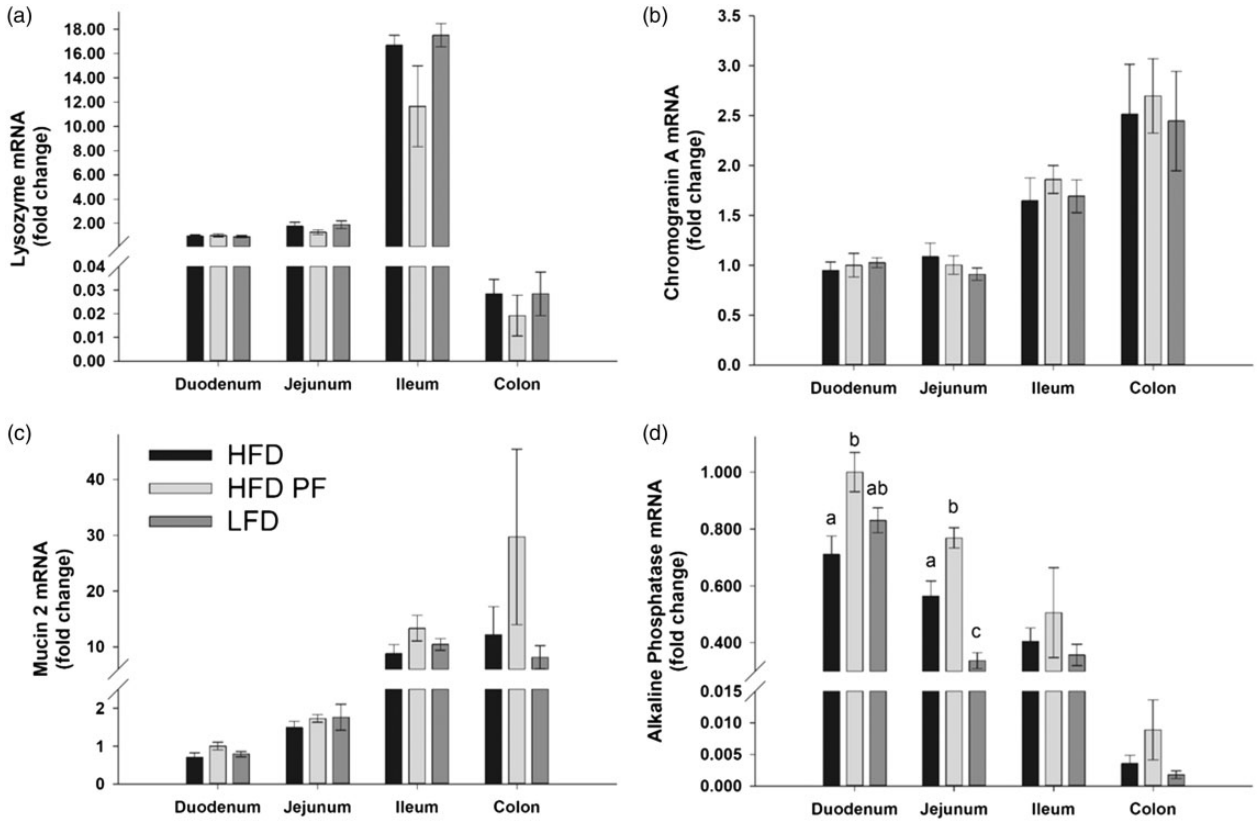

Figure 4. Gene expression of enzymes or secretory proteins of different intestinal epithelial cell types in intestinal segments (duodenum, jejunum, ileum and colon) collected from mice fed with HFD or LFD. Gene expression of lysozyme (Paneth cells) (a), chromogranin A (enteroendocrine cells) (b), mucin 2 (goblet cells) (c), and alkaline phosphatase (enterocytes) (d). Data are expressed as Mean ± SEM of fold change relative to HFD PF group in the duodenum ($n = 5$). Means with different letters indicate significantly different in each intestinal segment, $P < 0.05$.

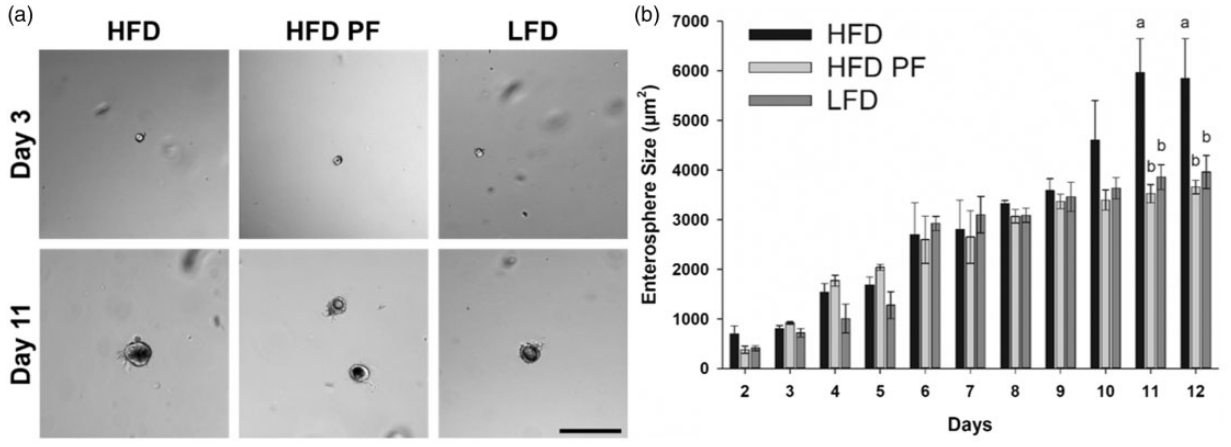

Figure 5. Representative images (a) and quantification of the size of enterospheres that developed from IESCs (b) isolated from mice fed with HFD or LFD. Scale bar, 200 μm. Data are expressed as Mean ± SEM ($n = 3$). Means with different letters indicate significantly different at each time point, $P < 0.05$.

been an adaptation in the PF animals to the feeding regimen in order to enhance the absorption of food. These mice are fed in a single HFD meal that is normally eaten in its entirety within an hour, instead of being able to eat the food *ad libitum* as in the HFD group. Moreover, the differences seen along the intestinal axis are likely because alkaline phosphatase-regulated lipid absorption mainly takes place in the proximal and not the distal intestine.[34] Thus, the interaction of diet, obesity, and the feeding regimen may alter the function of enterocytes in the proximal intestine and could potentiate the downstream effects of HFD-induced obesity. In addition, although we found that HFD-induced obesity increased goblet cell number, there were no differences in the expression of mucin 2, the major secretory mucin secreted by goblet cells, between groups. It is likely that obesity-induced increases in goblet

cell number may contribute to the changes in the expression of other types of mucus proteins secreted by goblet cells, but not the expression of mucin 2.

We have replicated the findings that HFD-induced obesity results in lasting effects on IESC growth *in vitro*.[3,4] We show for the first time that this effect (1) occurs even when proliferation is investigated without concomitant differentiation and (2) was not driven by HFD alone and requires hyperphagia of the HFD and/or obesity. Although the delayed *in vitro* effect (significant differences between groups is not apparent until day 11) likely reflects the need for a threshold number of cells in the enterospheres to be present for statistical comparison, it is striking that the obesity-induced effect on IESC proliferation remains across multiple days of growth *in vitro*. Thus, there must be some intrinsic differences in how the "obese" versus "lean" stem cells adapt to a new environment. The retention of mechanisms of IESC proliferation after isolation and culture may be driven by *in vivo* high circulating levels of insulin and local release of insulin-like growth factor-1 (IGF-1), as suggested previously.[3,35,36] The long-term changes in insulin/IGF-1 receptor signaling in the IESCs may promote epigenetic modifications in the proliferation process, which might be retained in IESCs across generations of new cells *in vitro*, mechanisms that have yet to be studied. Regardless of the mechanism, it is not known whether this obesity-induced effect on IESC proliferation would also be maintained *in vivo* after weight loss or if animals were switched to a new diet. This might have far-reaching consequences for an individual as this may be a key factor in maintaining altered tissue growth and function associated with obesity. It is not clear, though, how the obesity-induced cellular adaptation may affect tissue growth or function.

Authors' contributions: WZ and MJD conceived and designed research; WZ and EAD performed experiments; WZ analyzed data; WZ and MJD interpreted data; WZ generated figures; WZ and MJD drafted manuscript; all authors were involved in editing and revising the manuscript, and had final approval of the submitted and published versions.

ACKNOWLEDGEMENTS

The authors are grateful to Kate Blackmore and Mary Kate Feldner for their contributions in cell isolation, and Shovik Patel and Angelina Mei for their contributions in tissue processing.

DECLARATION OF CONFLICTING INTERESTS

The author(s) declared no potential conflicts of interest with respect to the research, authorship, and/or publication of this article.

FUNDING

The author(s) disclosed receipt of the following financial support for the research, authorship, and/or publication of this article: This work was supported by USDA Hatch (to MJD) ILLU-538–926.

ORCID iD

Weinan Zhou http://orcid.org/0000-0001-9323-900X
Megan J Dailey http://orcid.org/0000-0003-4587-2307

REFERENCES

1. Barker N, Bartfeld S, Clevers H. Tissue-resident adult stem cell populations of rapidly self-renewing organs. *Cell Stem Cell* 2010;**7**:656–70
2. Dailey MJ. Nutrient-induced intestinal adaption and its effect in obesity. *Physiol Behav* 2014;**136**:74–8
3. Mah AT, Van Landeghem L, Gavin HE, Magness ST, Lund PK. Impact of diet-induced obesity on intestinal stem cells: hyperproliferation but impaired intrinsic function that requires insulin/IGF1. *Endocrinology* 2014;**155**:3302–14
4. Beyaz S, Mana MD, Roper J, Kedrin D, Saadatpour A, Hong SJ, Bauer-Rowe KE, Xifaras ME, Akkad A, Arias E, Pinello L, Katz Y, Shinagare S, Abu-Remaileh M, Mihaylova MM, Lamming DW, Dogum R, Guo G, Bell GW, Selig M, Nielsen GP, Gupta N, Ferrone CR, Deshpande V, Yuan GC, Orkin SH, Sabatini DM, Yilmaz OH. High-fat diet enhances stemness and tumorigenicity of intestinal progenitors. *Nature* 2016;**531**:53–8
5. Baldassano S, Amato A, Cappello F, Rappa F, Mule F. Glucagon-like peptide-2 and mouse intestinal adaptation to a high-fat diet. *J Endocrinol* 2013;**217**:11–20
6. Mao J, Hu X, Xiao Y, Yang C, Ding Y, Hou N, Wang J, Cheng H, Zhang X. Overnutrition stimulates intestinal epithelium proliferation through beta-catenin signaling in obese mice. *Diabetes* 2013;**62**:3736–46
7. Sclafani A. Dietary-induced overeating. *Ann N Y Acad Sci* 1989;**575**:281–9; discussion 90–1
8. Hill JO, Peters JC. Environmental contributions to the obesity epidemic. *Science* 1998;**280**:1371–4
9. Li H, Kek HC, Lim J, Gelling RW, Han W. Green tea (-)-epigallocatechin-3-gallate counteracts daytime overeating induced by high-fat diet in mice. *Mol Nutr Food Res* 2016;**60**:2565–75
10. Cani PD, Bibiloni R, Knauf C, Waget A, Neyrinck AM, Delzenne NM, Burcelin R. Changes in gut microbiota control metabolic endotoxemia-induced inflammation in high-fat diet-induced obesity and diabetes in mice. *Diabetes* 2008;**57**:1470–81
11. Guo J, Jou W, Gavrilova O, Hall KD. Persistent diet-induced obesity in male C57BL/6 mice resulting from temporary obesigenic diets. *PLoS One* 2009;**4**:e5370
12. Blackmore K, Zhou W, Dailey MJ. LKB1-AMPK modulates nutrient-induced changes in the mode of division of intestinal epithelial crypt cells in mice. *Exp Biol Med* 2017;**242**:1490–8
13. Sato T, Clevers H. Primary mouse small intestinal epithelial cell cultures. *Methods Mol Biol* 2013;**945**:319–28
14. Wang F, Scoville D, He XC, Mahe MM, Box A, Perry JM, Smith NR, Lei NY, Davies PS, Fuller MK, Haug JS, McClain M, Gracz AD, Ding S, Stelzner M, Dunn JC, Magness ST, Wong MH, Martin MG, Helmrath M, Li L. Isolation and characterization of intestinal stem cells based on surface marker combinations and colony-formation assay. *Gastroenterology* 2013;**145**:383–95.e1–21
15. Yin X, Farin HF, van Es JH, Clevers H, Langer R, Karp JM. Niche-independent high-purity cultures of Lgr5+ intestinal stem cells and their progeny. *Nat Methods* 2014;**11**:106–12
16. Lalles JP. Intestinal alkaline phosphatase: multiple biological roles in maintenance of intestinal homeostasis and modulation by diet. *Nutr Rev* 2010;**68**:323–32
17. Bel S, Pendse M, Wang Y, Li Y, Ruhn KA, Hassell B, Leal T, Winter SE, Xavier RJ, Hooper LV. Paneth cells secrete lysozyme via secretory autophagy during bacterial infection of the intestine. *Science* 2017;**357**:1047–52
18. Kim T, Tao-Cheng JH, Eiden LE, Loh YP. Chromogranin A, an "on/off" switch controlling dense-core secretory granule biogenesis. *Cell* 2001;**106**:499–509
19. Engelstoft MS, Egerod KL, Holst B, Schwartz TW. A gut feeling for obesity: 7TM sensors on enteroendocrine cells. *Cell Metab* 2008;**8**:447–9

20. Kim YS, Ho SB. Intestinal goblet cells and mucins in health and disease: recent insights and progress. *Curr Gastroenterol Rep* 2010;**12**:319–30
21. Wolnerhanssen BK, Moran AW, Burdyga G, Meyer-Gerspach AC, Peterli R, Manz M, Thumshirn M, Daly K, Beglinger C, Shirazi-Beechey SP. Deregulation of transcription factors controlling intestinal epithelial cell differentiation; a predisposing factor for reduced enteroendocrine cell number in morbidly obese individuals. *Sci Rep* 2017;**7**:8174
22. Altmann GG, Leblond CP. Factors influencing villus size in the small intestine of adult rats as revealed by transposition of intestinal segments. *Am J Anat* 1970;**127**:15–36
23. Narisawa S, Huang L, Iwasaki A, Hasegawa H, Alpers DH, Millan JL. Accelerated fat absorption in intestinal alkaline phosphatase knockout mice. *Mol Cell Biol* 2003;**23**:7525–30
24. Goldberg RF, Austen WG, Jr, Zhang X, Munene G, Mostafa G, Biswas S, McCormack M, Eberlin KR, Nguyen JT, Tatlidede HS, Warren HS, Narisawa S, Millan JL, Hodin RA. Intestinal alkaline phosphatase is a gut mucosal defense factor maintained by enteral nutrition. *Proc Natl Acad Sci U S A* 2008;**105**:3551–6
25. Lawrie NR, Yudkin J. Studies in biochemical adaptation; effect of diet on the intestinal phosphatase of the rat. *Biochem J* 1949;**45**:438–40
26. Sefcikova Z, Hajek T, Lenhardt L, Racek L, Mozes S. Different functional responsibility of the small intestine to high-fat/high-energy diet determined the expression of obesity-prone and obesity-resistant phenotypes in rats. *Physiol Res* 2008;**57**:467–74
27. de La Serre CB, Ellis CL, Lee J, Hartman AL, Rutledge JC, Raybould HE. Propensity to high-fat diet-induced obesity in rats is associated with changes in the gut microbiota and gut inflammation. *Am J Physiol Gastrointest Liver Physiol* 2010;**299**:G440–8
28. Kaur M, Kaur J, Ojha S, Mahmood A. Dietary fat effects on brush border membrane composition and enzyme activities in rat intestine. *Ann Nutr Metab* 1996;**40**:269–76
29. Wahnon R, Cogan U, Mokady S. Dietary fish oil modulates the alkaline phosphatase activity and not the fluidity of rat intestinal microvillus membrane. *J Nutr* 1992;**122**:1077–84
30. Ognibene A, Pala L, Messeri G, Rotella CM, Berti P. Relations between intestinal alkaline phosphatase activity and insulin secretion in obese patients. *Clin Chem* 1997;**43**:1672–3
31. Khan AR, Awan FR, Najam SS, Islam M, Siddique T, Zain M. Elevated serum level of human alkaline phosphatase in obesity. *J Pak Med Assoc* 2015;**65**:1182–5
32. Kaliannan K, Hamarneh SR, Economopoulos KP, Nasrin Alam S, Moaven O, Patel P, Malo NS, Ray M, Abtahi SM, Muhammad N, Raychowdhury A, Teshager A, Mohamed MM, Moss AK, Ahmed R, Hakimian S, Narisawa S, Millan JL, Hohmann E, Warren HS, Bhan AK, Malo MS, Hodin RA. Intestinal alkaline phosphatase prevents metabolic syndrome in mice. *Proc Natl Acad Sci Usa U S A* 2013;**110**:7003–8
33. Malo MS. A high level of intestinal alkaline phosphatase is protective against type 2 diabetes mellitus irrespective of obesity. *EBioMedicine* 2015;**2**:2016–23
34. de Wit NJ, Boekschoten MV, Bachmair EM, Hooiveld GJ, de Groot PJ, Rubio-Aliaga I, Daniel H, Muller M. Dose-dependent effects of dietary fat on development of obesity in relation to intestinal differential gene expression in C57BL/6J mice. *PLoS One* 2011;**6**:e19145
35. Van Landeghem L, Santoro MA, Mah AT, Krebs AE, Dehmer JJ, McNaughton KK, Helmrath MA, Magness ST, Lund PK. IGF1 stimulates crypt expansion via differential activation of 2 intestinal stem cell populations. *FASEB J* 2015;**29**:2828–42
36. Andres SF, Santoro MA, Mah AT, Keku JA, Bortvedt AE, Blue RE, Lund PK. Deletion of intestinal epithelial insulin receptor attenuates high-fat diet-induced elevations in cholesterol and stem, enteroendocrine, and Paneth cell mRNAs. *Am J Physiol Gastrointest Liver Physiol* 2015;**308**:G100–11

(Received January 12, 2018, Accepted April 27, 2018)